

1.1. Particle-Wall Interactions

Often times, conditions for pipe flows and boundary layer flows can produce high concentrations of particles very near the wall. Several studies have shown such high concentrations at transverse positions on the order of the particle diameter for solid particles (Young and Hanratty, 1991; Kaftori *et al.* 1995; Young & Leeming, 1997) as well as for gas bubbles (Zun *et al.* 1992; Marie *et al.* 1997; Felton & Loth, 2001). In these cases, the consideration of particle wall interactions becomes crucial. In general, one may consider two types of forces that arise as a particle approaches a wall, i.e. hydrodynamic forces (a function of the continuous-fluid resistance due to the particle's proximity to the wall) and collision forces (which arise only from surface contact).

Rewrote introductory paragraph

Hydrodynamic Forces

Generally, the hydrodynamic forces are negligible for heavy particles ($\Psi \gg 1$) at high Reynolds numbers ($Re_p \gg 1$), but can be important for very small particles, e.g. aerosols in the respiratory tracts of mammals. These forces can be quite significant for particles with densities on the order of or much smaller than that of the continuum, e.g. blood cells in arteries or bubbly pipe flow.

For Stokesian flow, an analytical approximation for a particle moving in a quiescent fluid can be obtained for the small perturbation case in which the particle diameter (or largest dimension) is much smaller than the distance from the wall, i.e. $d \ll d_{norm}$ (Fig. 2.38). This approximation is valid for a general particle shape and gives rise to the following drag force corrections (Clift *et al.* 1978):

$$(f_{tang})^{-1} = 1 - \frac{9}{32} f_E \left(\frac{d}{d_{norm}} \right)$$

velocity parallel to wall, $d_{norm}/d \gg 1$ & $Re_p \ll 1$

$$(f_{norm})^{-1} = 1 - \frac{9}{16} f_E \left(\frac{d}{d_{norm}} \right)$$

velocity parallel to wall $d_{norm}/d \gg 1$ & $Re_p \ll 1$

in which f_{norm} and f_{tang} approach unity for $d_{norm} \gg d$, e.g. the corrections may be reasonably neglected for particles more than ten diameters away from the wall. Close to the wall (as d_{norm} approaches $d/2$), the tangential drag force increases, slowing the particle down while motion towards the wall or away from the wall is also hindered. Lin *et al.* (2000) found that the above approximations were reasonable for small (Brownian) particles of about 1 μm in diameter for values of $d_{norm}/d > 3$. Validity was not tested for positions closer to the wall because of experimental hinderances.

As a result of the above relations, the net drag force can be decomposed into components which are perpendicular and parallel to the wall, with corrections applied to each of the components. The resulting wall-corrected component of the drag coefficient is

Deleted: Particle interactions with walls can be a critical phenomenon for pipe flows and boundary layer flows. This is because certain conditions can yield a high concentration of particles very near the wall, e.g. at transverse positions on the order of the particle diameter itself as described in experiments with solid particle (Young and Hanratty, 1991; Kaftori *et al.* 1995; Young & Leeming, 1997) as well as with gas bubbles (Zun *et al.* 1992; Marie *et al.* 1997; Felton & Loth, 2001). In general, we will consider two types of forces which come about as a particle approaches a wall: first, hydrodynamic forces (a function of the continuous-fluid resistance due to the particle's proximity to the wall) and secondly, collision forces (which only come into effect when the particles contacts the surface).

Deleted: ¶

Deleted: In general

Deleted: are typically

Deleted: neglected

Deleted: and

Deleted: the surroundings

Deleted:

Deleted: With respect to hydrodynamic forces f

Deleted: gives

Deleted: where

Deleted: moving

Deleted: moving

Deleted: where

Deleted: $d/2$

Deleted: d_{norm}

Deleted: to slow

Deleted: ,

Deleted: while the experimental hindrances tended to be larger than the predicted values for positions closer to the wall.

Deleted: Thus

Deleted: the above respective

Deleted: ,

Deleted: e.g. the

Deleted: C_D

$$C_D = f_E f_{\text{norm}} \left(\frac{24}{Re_p} \right) \left(\frac{V_{p,\text{norm}}}{V_p} \right) + f_E f_{\text{tang}} \left(\frac{24}{Re_p} \right) \left(\frac{V_{p,\text{tang}}}{V_p} \right) \quad Re_p \ll 1$$

While the above approximations are derived assuming the particle diameter is much less than the distance to the wall, Young and Hanratty (1991) proposed a model for the modification of the quasi-steady viscous forces once the particle position from the wall (y) is on the order of the particle diameter for creeping flow. The modifications which were obtained using resolved-volume simulations of spherical particles in finite viscosity are based on the components of the particle motion perpendicular to the wall ($V_{p,\text{norm}}$) and parallel to the wall ($V_{p,\text{tang}}$) as noted in Fig. 2.38. The drag force functions were determined for particles with velocities parallel or perpendicular to the wall. The resulting drag correction factors can be reasonably approximated (within 2%) as:

$$f_{\text{tang}} = 1 + 0.35 \left(\frac{d}{d_{\text{norm}}} \right) \quad \text{velocity parallel to wall \& } Re_p \ll 1$$

$$f_{\text{norm}} = 1 + 1.1 \left(\frac{d}{2d_{\text{norm}} - d} \right) \quad \text{velocity perpendicular to the wall \& } Re_p \ll 1$$

where f_{norm} and f_{tang} exhibit similar behavior to the above analytical approximations.

(moved to next page)

For solid particles in the inviscid (Bernoulli) limit, a hydrodynamic wall interaction model based on potential flow for the wall imposition on the flow over the particle is given by Soo (1990). The modification includes both particle velocity and particle acceleration terms, and can thus be considered two components of a separate wall interaction force (instead of simply a modification of the drag force) where

$$F_{W,\text{tang}} = \left(\frac{1}{8} \right)^3 \pi \rho_f \left(\frac{d^6}{d_{\text{wall}}^4} \right) [d_{\text{norm}} dV_{p,\text{tang}}/dt - 3 V_{p,\text{norm}} V_{p,\text{tang}}]$$

$$F_{W,\text{norm}} = \left(\frac{1}{8} \right)^3 \pi \rho_f \left(\frac{d^6}{d_{\text{wall}}^4} \right) [2 d_{\text{norm}} dV_{p,\text{norm}}/dt - 3 (V_{p,\text{norm}})^2 - 3/2 (V_{p,\text{tang}})^2]$$

which can be thought of as generalized Bernoulli forces due to the presence of the wall.

For intermediate ranges of Re_p , the experimental study of Hallouin *et al.* (1998) examines the transition between the highly viscous regime and the inviscid regime for the (dominant) normal-wall drag corrections. The results indicate that the lubrication theory is quite reasonable for $Re_{p,\text{norm}} < 0.1$, whereas the particle is negligibly affected by the hydrodynamic viscous force for $Re_{p,\text{norm}} > 3$, where the normal Reynolds number is based on the particle velocity normal to the wall.

Deleted: becomes

Deleted: are based on

Deleted: They determined

Deleted:

Deleted: a

Deleted: moving

Deleted: and moving perpendicular to the wall, which can be

Deleted: simply

Deleted: moving

Deleted: moving

Deleted: have very

Deleted: s

Deleted: For lift, the Saffman wall corrections discussed by Wang *et al.* (1997) are qualitatively consistent with particle deposition rates and also show that lift decreases as the particle moves towards the wall) and can in fact change sign at about $d_{\text{norm}}/d=1.5$. This reversal may be consistent with the experimental results of Young and Hanratty (1991) which found significant concentrations of particles suspended about one particle diameter away from the wall for Re_p of order unity. Notably, the above models were derived for fixed particles (recall free particles can exhibit different behavior as discussed in §2.4).

Comment: May want to elaborate.

Deleted: ir

Deleted:

$$Re_{p,norm} = \rho_f V_{p,norm} d / \mu_f$$

Hallouin *et al.* (1998) also propose an empirical model for the range $0.1 > Re_{p,norm} > 3$.

A study of non-spherical particles has been conducted by Gavze & Shapiro (1996) that examines flows for various solid particle shapes. The researchers noted that the wall interactions can be complex or coupled, resulting in a modified resistance tensor in which acceleration in one direction can affect forces in all three directions. This can give rise to rotational translational coupling, i.e. the particles can have an oscillatory motion close to the wall due to changes in the aspect ratio orientation brought about by the wall force. It is notable that the researchers found that the effect of the wall decreased as the particles non-sphericity increased. As such, the spherical wall corrections can be considered as an upper-bound to the corrections for non-spherical particles.

For bubbles, measurements of the tangential velocity component for bubbles sliding along a tilted wall ($d_{norm}/d \sim 0.5$) with Re_p in the range of 50 to 200 in clean quiescent water by Tsao & Koch (1997) yielded a drag coefficient consistent with that of the contaminated formula given in §2.3. This suggests, that f_{tang} is on the order of unity, which may be attributed to the presence of a thin lubrication film between the bubble and the wall that appears to counterbalance the enhanced drag force due to the wall proximity.

With respect to possible lift influence, there are no direct measurements. However, the suspension phenomenon described above for particles at locations of $d_{norm}/d \sim 0.6$ was also noted at $Re_p \gg 1$ for spherical bubbles by Felton & Loth (2001) and for ellipsoidal by Marie *et al.* (1997), thus indicating there may be a similar lift reversal effect for these conditions.

For lift, the Saffman wall corrections discussed by Wang *et al.* (1997) are qualitatively consistent with particle deposition rates and also show that lift decreases as the particle moves towards the wall) and can in fact change sign at about $d_{norm}/d = 1.5$. This reversal may be consistent with the experimental results of Young and Hanratty (1991) which found significant concentrations of particles suspended about one particle diameter away from the wall for Re_p of order unity. Notably, the above models were derived for fixed particles (recall free particles can exhibit different behavior as discussed in §2.4). While there hasn't been any direct measurements of the influence of particle wall interactions on lift, additional confirmation has been obtained for particles at locations of $d_{norm}/d \sim 0.6$ and $Re_p \gg 1$ for spherical bubbles by Felton & Loth (2001) and for ellipsoidal by Marie *et al.* (1997), thus indicating there may be a similar lift reversal effect for these conditions.

Inviscid Collision Forces

Generally, the collision of heavy particles ($\Psi \gg 1$) at high Reynolds numbers ($Re_p \gg 1$) is an inviscid process for which two types of models for the mechanical interaction can be considered: a hard-particle model and a soft-particle model. In the former, no deformation of the particle is considered; whereas in the latter, the details of the particle motion and/or wall motion are described as a spring and dashpot system. Because the details of such a system are typically empirical and test condition specific, most numerical methods which use the point-

Comment: May want to state what it is, or omit the sentence.

Deleted: With respect to

Deleted: ,

Deleted: examined

Deleted: and n

Deleted: i.e. can give rise to

Deleted: (where

Deleted:)

Deleted: such that

Deleted: since the wall force will modify as the aspect ratio inclination to the wall changes.

Deleted: However, they generally

Deleted: typically

Deleted: ~1

Deleted: . This is

Deleted: the

Deleted: which may

Deleted:

Comment: Here I have attempted to move the discussion of lift after the discussion of drag.

Deleted: where

Deleted: very

volume approach assume a hard-particle model. The hard-particle approach is characterized by simple expressions relating the change in wall-normal, wall-tangential, and angular components of the particle velocity. Here, the change in mass of the particle (e.g. particle breakup or droplet splatter) is not considered, so the wall-normal and wall-tangential components of the velocity can be written as a function of their respective coefficients of momentum restitution, e_{norm} and e_{tang} , such that

$$\begin{aligned} V_{p,norm}^{out} &= -e_{norm} V_{p,norm}^{in} \\ V_{p,tang}^{out} &= e_{tang} V_{p,tang}^{in} \end{aligned}$$

For a perfectly elastic inviscid collision with $\Psi \gg 1$, $e_{norm}=e_{tang}=1$; for an enforced stick or slide condition, $e_{norm}=0$. The coefficients of momentum restitution allow the determination of the rebound angle. Again, for a perfectly elastic inviscid collision the angle of impingement will equal the angle of reflection indicating a specular collision.

For the tangential restitution of solid spherical particles, Crowe *et al.* (1998) present details for the wall-interaction for finite angular velocity of the particle; however, we may typically neglect the angular velocity effects if the wall rotation parameter ($a_{p,wall}$) based on relative velocity to the wall is small or if $\Psi \gg 1$. In such cases, the tangential component of velocity is affected by the coefficient of dynamic skin friction (f) between the particle and the wall surface and the normal component of velocity as follows:

$$\begin{aligned} e_{tang} &= 5/7 && \text{for } |V_p/V_{p,norm}|^{in} > 3.5 f (e_{norm} + 1) \\ e_{tang} &= 1 + f (e_{norm} + 1) (V_{p,tang}/V_{p,norm})^{in} && \text{for } |V_p/V_{p,norm}|^{in} < 3.5 f (e_{norm} + 1) \end{aligned}$$

where f is typically obtained experimentally or empirically.

For non-spherical solid particles, Hamed (1988) and Hamed & Kuhn (1993) examined coefficients of restitution for micron sand particles (150 micron mean diameter) and fly-ash particles (15 micron mean diameter) for various impingement angles. The non-spherical particles exhibited significant statistical variations in rebound angle and velocity owing to their irregular shape. The e_{norm} for both cases was not constant (as is derived for spherical particles) but roughly decreased from 0.6 to 0.3 as the impingement angle from the wall increased from 15 degrees from the wall to 80 degrees. For these same conditions the e_{tang} was nearly constant at 0.45, but again the standard deviation was a significant fraction of the mean. The study of Tsirkunov & Panfilov (1998) discussed issues associated with surface strength and roughness and proposed an empirical model to account for these effects.

Viscous Collision Forces

In cases for which the particle density is lower (i.e. ~ 1 or less) and the Reynolds number can no longer be considered large ($Re \sim 1$ or less), the coefficient of restitution may be significantly reduced by viscous effects. For example, recent experimental results for steel particles dropped in a liquid by Zenit *et al.* (1999) have shown that $e_{norm} \sim 1$ is only reasonable for smooth hard spheres and a solid wall when the velocity relative to the wall is high. To

Deleted: Since we are not considering
Deleted: ,

Deleted: we have
Deleted:
Deleted: we have
Comment: This may further elucidate the coefficients?

Deleted: for
Deleted: . H

Deleted:

Deleted: about
Deleted: of
Deleted: s

Deleted: where
Deleted: particles
Deleted: are no longer heavy and at high Reynolds numbers
Deleted: are insignificant
Deleted: of
Deleted: relative

characterize the magnitude of the inertial to viscous forces in a collision, a normal-reflection Stokes number is employed, St_{norm} , which is the ratio of Stokesian response time to the time scale for the wall interaction (which is proportional $d/V_{p,norm}^{in}$), i.e.

$$St_{norm} = \frac{\mu_f}{\rho_p d} \frac{d}{V_{p,norm}^{in}} = (Re_{p,norm}/9)(\Psi+1/2)$$

Comment: It would be good to see the development of this equation.

The Zenit *et al.* (1999) results are shown in Fig. 2.39 where it can be seen that $e_{norm,visc}$ tends to the inviscid value, e_{norm} (ca. 1) for $St_{norm} \gg 1$, but $e_{norm,visc}$ decreases with St_{norm} due to the viscous interactions. This trend has also been observed in a more recent experimental study for millimetric bubbles in a turbulent boundary layer (Loth & Felton, 2001). The data points shown in Fig. 2.39 would suggest that bubble collisions are more efficient (elastic) than those for solid particles at a given St_{norm} . While this is not necessarily the case since there are significant flow differences between the two experiments (pure normal reflections in a quiescent fluid vs. angled reflections in a turbulent fluid), recent measurements of Tsao & Koch (1997) have given credence to this phenomenon by showing that millimetric bubbles can have significantly larger reflections from hard surfaces than that expected for an elastic collision. This is attributed to a complex exchange of surface tension and inertial forces.

Deleted: is

Deleted: Also shown in this figure are the present experimental data for millimetric bubbles in a turbulent boundary layer of Loth & Felton (2001), where we note that there is also a decrease in for decreasing St_{norm} . This again suggests viscous effects become more important as St_{norm} decreases.

Deleted: It is interesting that the

Deleted: reflections

Deleted: appear to be

Deleted: the

Deleted: for

Deleted: This

Deleted: may

Deleted: be

Deleted: actual

Deleted:).

Deleted: However such a phenomenon, if true, would be consistent with

Deleted: which s

Deleted: ed

Deleted: due

Comment: It would be good to include an estimate for the elasticity parameter for each of the data sets shown in Fig. 2.39.

Deleted: where

Deleted: ir

Deleted: that the a second important

Deleted: parameter

Deleted: is

Deleted: while

Deleted: where

Deleted: to

Deleted: was

Deleted: H

Deleted: With respect to

Also shown on the plot is a data curve from the experiments of Davis (2002) in which steel particles were dropped onto a thick quartz plate (dashed line) and a thin quartz plate (dotted line) with a thin viscous liquid. The results indicate the importance of a second non-dimensional quantity, i.e. the elasticity parameter

$$= \frac{\sqrt{2}}{\pi} \mu_f d^{3/2} V_{p,norm}^{in} [(1-\nu_p^2)/Y_p + (1-\nu_w^2)/Y_w] (d_{wall}^{in})^{3/2}$$

where ν_p and ν_w are the Poisson's ratio for the particle and the wall, Y_p and Y_w are the Young's modulus for the particle and the wall, and $V_{p,norm}$ is the approach velocity at a distance d_{wall}^{in} from the wall. One important finding is that there is a critical Stokes number for particle rebound ($St_{norm,cr}$) below which the viscous dissipation is too great for a significant rebound. This critical Stokes rebound value is a function of the elasticity parameter, e.g. $St_{norm,cr} \sim 1$ for $\epsilon = 10^{-2}$ and $St_{norm,cr} \sim 5$ for $\epsilon = 10^{-8}$. An empirical expression for this relationship has been given by Davis *et al.* (2002) as

$$St_{norm,cr} = 0.40 \ln(1/\epsilon) - 0.20$$

Above this critical value, the coefficient of restitution increases with rebound Stokes number; however, the manner of the increase depends on the parameter of elasticity, e.g. the thin plate results of Davis *et al.* (2002) shown in Fig. 2.39 give lower coefficient of restitution values as compared to that of the thick plate. This result indicates again that bubbles may have higher restitutions than spherical particles at equivalent rebound Stokes numbers. For solid particles, Davis *et al.* (2002) tested a model whereby the kinetic energy associated with motion towards the wall was proportionally reduced by the viscous dissipation so that

$$e_{norm,visc} \sim e_{norm} (1 - St_{norm,cr} / St_{norm})$$

$$e_{norm,visc} \sim 0$$

$$\text{for } St_{norm} > St_{norm,cr}$$

$$\text{for } St_{norm} < St_{norm,cr}$$

The results of several experiments are shown in Fig. 2.40 using the above expressions for $St_{\text{norm,cr}}$ and $e_{\text{norm,visc}}$, where the agreement is generally good. For the spherical bubble results of Felton & Loth (2001), use of a $St_{\text{norm,cr}}$ of about unity would give results within the experimental spread of Fig. 2.40.

1.2. Mass-Transfer Blowing Effects

It has been observed that a mass flux across the particle / continuum interface can cause the drag force to be reduced – a phenomenon that is often referred to as the blowing effect. This occurs as a result of the modification of the normal velocity boundary condition as shown in Fig. 2.41a (i.e. consistent with a blowing or suction boundary which can reduce the drag on spheres and airfoils). The net reduction can be expressed as a correction to the drag coefficient and is approximately independent of the sign of the radial velocity at the particle surface (V_{bl}). Miller & Bellan (1999) obtained an empirical expression for spherical particles which was consistent with the resolved-volume simulation data of Cliffe & Lever (1985) for $Re_p < 100$ and $Re_{bl} < 10$:

$$f_{bl}^{-1} = 1 + [0.09 + 0.077 \exp(-0.4 Re_p)] |Re_{bl}|^{0.4 + 0.77 \exp(-0.04 Re_p)}$$

where the particle blowing Reynolds number is defined as $Re_{bl} = (\rho_f d V_{bl} / \mu_f)$. As expected, the reduction in drag force is only a function of the blowing Reynolds number.

A different effect related to mass transfer occurs when a gradient in vapor concentration leads to a diffusion driven asymmetric mass flux at the particle surface causing net motion of the particle – a phenomenon sometimes referred to as diffusiophoresis. A schematic showing the asymmetric blowing due to a gradient in vapor pressure is shown in Fig. 2.41b. For example, a droplet will tend to be repelled by an evaporation (humid wall) since it can evaporate faster on the other side of the particle (or condense less on the near side of the particle). Other continuous-field gradients can cause such asymmetric blowing, including gradients in temperature, density or pressure. The relationship between these parameters and the evaporation rate causes a coupling between conserved quantities of mass and energy that must be accounted for in the analysis of many multi-phase processes.

Deleted: The effect of

Deleted: . This

Deleted: sometimes

Deleted: due to

Comment: How specifically does this boundary condition modification lead to a decreased drag?

Comment: Doesn't suction on a flat plate sometimes increase the drag to prevent early BL separation?

Comment: Isn't this relation also a function of the particle Reynold's number?

Deleted: However, a gradient

Deleted: can cause

Deleted: which will cause a

Deleted: . This is

Deleted: (forces due to diffusion of mass across a particle interface)

Deleted: However, o

Deleted: filed

Deleted: ticles

Inserted: ticles and the evaporation rate causes a coupling between conserved quantities of mass and energy that must be accounted for in the analysis of many multi-phase processes.

Deleted: since these are related to the overall evaporation rate (Clift *et al.* 1978).

1.3. Thermophoresis and other Continuous-Field Gradient Effects

Many of the previous sections dealt with modifications of the particle equation of momentum associated with the hydrodynamic flow gradients (associated with velocity and pressure). It should be noted that turbophoresis is an effect which is inherently included in the point-force model as long as the flow around the particle is fully-resolved. However, in the case of Reynolds-averaging (and other eddy-averaging methods), this effect may need to be modeled to be properly incorporated. A discussion of models will be included in §3.3.4. As mentioned in the previous section, some multi-phase flows require the evaluation of forces arising from non-hydrodynamic gradients which can be important to the net acceleration of the particle. These forces include: thermophoresis (forces due to temperature gradients), photophoresis (forces due to light beam intensity), and electrophoresis (due to a potential across the field). In general, these effects tend to be negligible except for specialized conditions of very small particles (e.g. less than a micron) in low density gasses (caused by vacuum conditions or high temperatures).

Deleted: In the above sections, resulting

Deleted: were noted

Deleted: automatically

Comment: Could this possibly go in a footer?

Deleted: (This seems like it could go in a footer).

Inserted: (This seems like it could go in a footer). As mentioned in the previous section, some multi-phase flows require the evaluation of forces arising from non-hydrodynamic gradients which can be important to the net acceleration of the particle. These forces include:

Deleted: ¶

¶ In addition to the effects on the particle force by the above mentioned hydrodynamic gradients, there are additional effects associated with other gradients which can be important to the net acceleration of the particle and some of these will be briefly summarized in this section. This will include

Deleted: ed

Deleted: generally

Thermophoresis

Thermophoretic forces arise when there is a net momentum flux to a particle in the continuous phase that arises from temperature gradients. The hot side of a macroscopic particle experiences collisions from fluid particles with higher molecular velocities as compared to that of the cool side according to kinetic gas theory. The net result is particle movement opposite and parallel with the temperature gradient in a fashion analogous to heat conduction. To put it simply, if the temperature gradients across the particle are sufficiently large, thermophoresis causes a macroscopic particle to move away from a hot wall, toward a cold one (see optional Figure 1). Note, this condition is quite different from that due to a pressure gradient in an isothermal flow, such that the two effects may be super-imposed to obtain the effective force on a particle.

There are a number of important applications in which thermophoretic forces play an important role, including plasma flows in which the temperature gradients across the particle are very large. Another would be the erosion process in combustors and heat exchangers in which particles are drawn toward a cool wall in a very hot flow causing fouling or erosion over time. Also, the radiative transfer from sooting particles can be strongly influenced by thermophoresis because of the large gradients caused by continuum emission, resulting in particle movement and preferential concentrations, yielding a very complicated coupling between the energy and momenta equations. Finally, the fabrication of high yield processors is highly dependant on thermophoresis because of the repulsion and or deposition of impurities on the wafer as it heats up during fabrication.

Deleted: The thermophoretic effect caused by temperature gradients in the continuous fluid surrounding the particle arises due to the gradient of the kinetic energy of the surrounding molecules. Such a gradient, results in higher molecular velocities on one side of a particle than on the other. Note, this condition is different from that due to a pressure gradient in an isothermal flow, such that the two effects may be super-imposed to obtain the effective force on a particle. ¶

Deleted: n

Deleted: ¶

Deleted: is parallel to the direction of the temperature gradient and

Comment: Here it might be good to restate the mean free path so as to see the functional relationships.

For large Knudsen number ($\omega \gg d$), the thermophoretic force is given (Soo, 1990) for an accommodation coefficient of unity as

$$\mathbf{F}_{\nabla T} = -\frac{1}{8} \pi \omega \rho_f d^2 R_f \nabla T \quad \text{for } Kn_p \gg 1$$

and is generally negligible for continuum flow conditions (i.e. for conditions in which the particle diameter is greater than 1 micron because of the dominance of drag associated with the terminal velocity). For intermediate Knudsen numbers (the transitional regime), the differences between the temperature gradient of the particle and of the gas become significant such that the ratio of the particle and surrounding fluid thermal conductivities $k_{p/f}$ becomes important (Epstein, 1929)

$$F_{\nabla T} = -\frac{9}{2} \mu_f d (2 \pi R_f / T_f)^{1/2} (\nabla T) k_{p/f} / (1 + 2 k_{p/f}) \quad \text{for } Kn_p \sim 1$$

Deleted: (Here it might be good to restate the mean free path so as to see the functional relationships). ¶

Inserted: (Here it might be good to restate the mean free path so as to see the functional relationships).

Deleted: It can be seen that the higher kinetic energy side of the particle causes movement in the other direction. ¶

Deleted: via

Deleted: via

Crowe *et al.* (1998) discusses empirical corrections to the above expression based on the ratio of the surrounding fluid and particle thermal conductivities $k_{f/p}$. A more recent expression given by Wu (2003), allows evaluation of the thermophoretic force over a more general range of Knudsen numbers, in which

$$F_{\nabla T} = -\frac{9\pi}{2\rho_f} \mu_f^2 d (\nabla T/T) (2.2 Kn_p + k_{f/p}) / [(1 + 4.4 Kn_p + 2k_{f/p}) (1 + 3 Kn_p)]$$

for $Kn_p \sim 1$ & $\gg 1$

Deleted: is

Deleted: where

The trends of these results are shown in Fig. 2.42 for a particle in STP air conditions subjected to a temperature gradient of 1% across the particle diameter and a Stokesian drag force. It can be noted that particles greater than a micron in size will tend to have movements less than one diameter per second. For particles above one micron in STP air (for which the ratio of conductivities becomes significant), the thermophoretic velocities are at least an order of magnitude smaller than the terminal velocities of the particles, indicating that the gravitational forces are much stronger than the thermophoretic forces. This has also been verified in a recent study examining the critical diameter of particles above which all are deposited in chemical vapor deposition (MacGibbon, Busnaina, Fardi, 1999). In this study, the authors verified experimentally and theoretically that thermophoretic forces greatly inhibit impurity deposition for particles between 0.01 and 1 micron when a hot wafer is in a cool vapor deposition shower. The authors' analysis considered the equation of motion for spherical particles using the BBO equation with included thermophoretic and Brownian terms. It is notable that for very small particle sizes (0.01 micron or less), the Brownian motion of particles can become quite significant, requiring an order of magnitude analysis between forces arising from random molecular motion and forces arising from molecular collisions due to temperature gradients (thermophoresis).

Deleted: such

Deleted: is

Deleted:

Deleted: '

(Here follows a brief alternate discussion of thermophoretic forces for optional inclusion.)

In a recent study using the Direct Simulation Monte Carlo (DSMC), Gallis, et. al. (2001), simulated the thermophoretic force for a number of regimes for comparison with previous theoretical results. The authors found that the pressure can be an important factor in

determining the thermophoretic force for low pressure conditions. Here, two Knudsen numbers were formulated according to three characteristic length scales, i.e. particle radius, R_p , mean free path, ϖ , and system size, L (which is the distance between two plates establishing the thermal gradient. The particle and system Knudsen numbers are given by:

$$Kn_p = \varpi / R_p \quad Kn_s = \varpi / L$$

For all of the analysis conducted in the study, the particle Knudsen number was assumed to be much larger than one, indicating that the particle radius is much smaller than the mean free path. For different limits of the system Knudsen number that corresponds to the ratio of the mean free path to the system size, theoretical regimes for the thermophoretic forces have been formulated:

Formatted: Font: Not Italic, No underline

Continuum Gas (Waldman)

$$F_{con} = -\frac{16}{15} \pi^{\frac{1}{2}} \beta R_p^2 k_f \frac{dT}{dx}, \quad \beta = \sqrt{\frac{m}{2kT}} \quad (Kn_p \rightarrow \infty, Kn_s \rightarrow 0)$$

Formatted: Lowered by 13 pt

When the mean free path is small compared to the system size, the domain can be considered continuous. The above formulation by Waldman is directly proportional to the temperature gradient and the thermal conductivity, but is independent of pressure or particle density (so long as the Knudsen number criteria is met).

Free-Molecular Gas (Brock, Phillips, Torczynski)

$$F_{FM} = -\left(\frac{3}{2} \pi R_p P\right) \left(\frac{T_H^{\frac{1}{2}} - T_C^{\frac{1}{2}}}{T_H^{\frac{1}{2}} + T_C^{\frac{1}{2}}} \right), \quad P = nkT_C^{\frac{1}{2}} T_H^{\frac{1}{2}} \quad (Kn_p \rightarrow \infty, Kn_s \rightarrow \infty)$$

When the mean free path is large compared to the system size, the domain can be considered to be a free-molecular gas. In this case, an altered temperature gradient has been formulate to correct for small temperature differences. The significant result is that the thermophoretic force is linearly dependant on the free molecular pressure on the walls.

Transitional Regime (Phillips)

$$F_{Ph} = -\left(\frac{32}{15\pi}\right) \left(\frac{\pi R_p^2}{\bar{c}}\right) \left(\frac{K(T_H - T_C)}{L}\right) \left(\frac{45\pi N + N^2}{1 + N + N^2}\right) \quad (Kn_p \rightarrow \infty, Kn_s \rightarrow O(1))$$

$$N = \frac{14}{15} \frac{L \rho \bar{c}}{2\mu}, \quad \bar{c} = \sqrt{\frac{8kT}{\pi m}}$$

When the mean free path is on the order of the system size, the thermophoretic force becomes very difficult to accurately predict. The theoretical result presented above is the weakest of the three. The relation shows a weaker pressure dependence with an explicit dependence on the mean molecular speed.

Using the DSMC method, Gallis, et. al. were able to provide very accurate simulations of the thermophoretic force for comparison with the theoretical regimes. Through the use of precise probabilistic functions to determine the motion of many "fluid" particles, a precise relation for the thermophoretic force could be determined. Optional Figure 2 shows results for

the DSMC simulations as compared to the aforementioned theory for each of the three regimes. The results show good agreement between simulations and theory for the continuum and free-molecular regimes, but the weakness of the result for the theoretical transitional regime is apparent (error as much as 20%). For the free molecular regime, one can see the linear (on the log scale) dependence of the thermophoretic force with pressure, while for the continuum regime, the pressure dependence has vanished, indicating that once there are sufficient numbers of molecules colliding with the macroscopic particle to establish a continuum, the pressure effect becomes negligible.

These results have major implications for the manufacture of processors because of the near vacuum conditions at which they are fabricated. The thermophoretic force that repels impurities from the chip surface is relied upon to provide high yields. Knowing the influence of pressure on the effect is tantamount to good production.

Formatted: Font: Not Italic, No underline

(End of optional inclusion)

Photophoresis and Electrophoresis

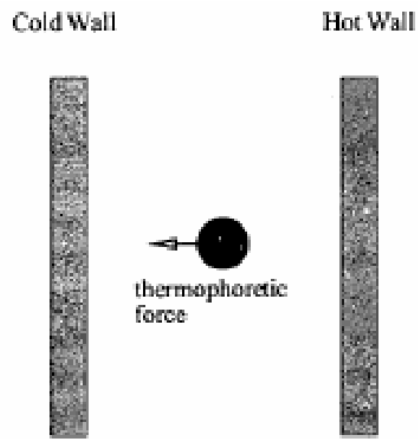
The photopheretic effect is due to the asymmetry of photon fluxes at the particle surface. Soo (1990) describes an empirical correction for a beam of light having an intensity impacting only one side of a spherical particle. The expression is based on rarefied flow conditions with Knudsen numbers of order unity. For electrophoresis, the force on the particle (sometimes called the Coulomb force) is simply the product of the charge on the particle and the electric field intensity. An electric field may be used to charge the particle itself as well as to supply the electromotive force. This phenomenon forms the basis for an electrostatic precipitator. (Crowe *et al.* 1998).

Deleted: e

Deleted: The particle may be charged using an electric field and is the basis for an electrostatic precipitator

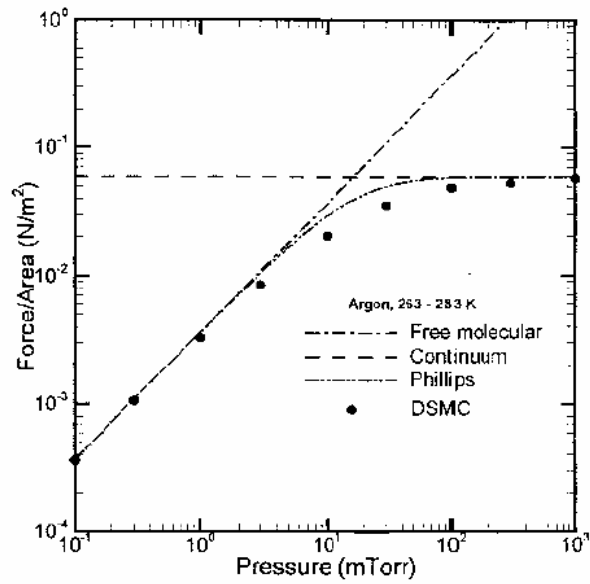
Deleted: n

As with any other force arising from hydrodynamic gradients, it is crucial that an order of magnitude analysis be conducted for all surface and body forces arising from non-hydrodynamic gradients in order to properly determine the dynamics of particle motion.



Formatted: Centered

Optional Figure 1. The thermophoretic force on a particle is oriented parallel to and opposing the temperature gradient.



Formatted: Font: 14 pt, Bold

Optional Figure 2. DSMC and theoretical results for thermophoretic force in each of three regimes arising from changes in pressure.